Met. Mater. Int., Vol. 20, No. 4 (2014), pp. 719~726
doi: 10.1007/s12540-014-4017-y

Effects of Processing Parameters on Elastic Deformation of the Coil During the Thin-Strip Coiling Process

Won-Woong Park[1], Dong-Kyu Kim[1], Yong-Taek Im[1,2,*], Hyuck-Cheol Kwon[3], and Myung-Sik Chun[3]

[1]KAIST, School of Mechanical, Aerospace and Systems Engineering, Daejeon 305-701, Korea
[2]KIMM, Office of the President, Daejeon 305-343, Korea
[3]POSCO Technical Research Laboratories, Rolling & Instrumentation Research Group, Gwangyang, Jeonnam 545-090, Korea

(received date: 11 August 2013 / accepted date: 12 November 2013)

It is well known that axial inhomogeneity of the stress distribution within a thin-strip causes defects such as edge waves and center buckling during the thin-strip coiling process. In the current study, an analytical model was utilized to investigate the effects of processing parameters such as strip crown, spool geometry, and coiling tension on the elastic stress distribution and deformation of the strip during the coiling process. In the present investigation, the elastic modulus was introduced as a function of temperature and axial distance for better simulation of the process. According to the present analyses, it was found that improvement of the strip flatness might be achieved by suppressing the strip crown, increasing the thickness of the spool with the shape of a swollen hollow cylinder, and lowering the coiling tension with transient increase at the beginning stage of the coiling process only. This study will be helpful for better understanding of identifying the proper processing parameters during the coiling process.

Keywords: metals, rolling, deformation, strip coiling, flatness defect

1. INTRODUCTION

The evolution of modern manufacturing technology demands continually increasing international competitiveness of manufacturing processes and products, requiring lower manufacturing costs with better product quality due to sustainability and environmental issues. In this regard, the production of high-strength hot-rolled thin-coils is of importance in a steel mill for applications in the transportation industry. Since manufacturing of a hot-rolled thin-strip consists of several stages, roughing, rolling, cooling, and coiling, the cold shape of the thin-strip has an arbitrary irregular thickness profile such as ∩, ∪, M, and W shapes. It is not easy to predict the cold shape of the thin-strip, however, because of variations in processing facilities and operation conditions, as reported by Jung and Im [1,2].

A strip crown, a difference between the center and the edge thicknesses along the axial direction in the rolled strips, can develop owing to several factors such as roll bending, wear, and thermal distortion [3]. During the strip coiling process, the strip crown formed by the rolling process incurs axial inhomogeneity of the deformation, causing flatness defects in the coil [4]. In order to satisfy customer requirements for strip flatness, the strip is usually cut, welded, and recoiled in the recoiling line. However, even after the recoiling line, flatness defects sometimes remain, especially in high-strength hot-rolled coils. For prevention of such flatness defects, it is necessary to predict the deformation of the coil depending on the processing parameters to better understand the mechanism of possible defect formation.

In order to simulate deformation mechanics of the coiling process, Sims and Place [5] proposed a stress model of the coil under the assumption that the coil was a hollow cylinder with axial symmetry. Miller and Thornton [6] and Sarban [7] introduced a semi-analytical model and a finite element method, respectively, to calculate the 3D stress distribution within the coil. However, physical clearance between each coiled wrap due to the strip crown was not considered in their models as a cause of the axial inhomogeneity. Yanagi *et al.* [8] suggested an analytical model based on piling a thick cylinder (the coil) with thin-walled cylinders (the new coiling strips) to consider the inhomogeneous deformation of the cold-rolled thin-strip in the axial direction due to the strip crown and the clearance. Through comparison with the measured circumferential strain distribution, their results revealed that the strip flatness of the cold-rolled thin-strip could be improved by suppressing the strip crown and lowering the coiling tension intensity [8]. It should be noted, however, that the effect of the temperature

*Corresponding author: ytim@kaist.ac.kr

on the mechanical properties such as Young's modulus was not included in their analysis.

In the present study, the effects of processing parameters on the flatness of a hot-rolled thin strip during the coiling process are investigated through a stress analysis by revisiting the elastic model introduced by Yanagi *et al.* [8]. To determine the effect of each processing parameter more precisely, the stress distribution within the coil was calculated with varying not only the strip crown and coiling tension intensity but also with the spool geometry and applied transient coiling tension. In addition, the temperature dependent Young's modulus, provided by POSCO, was introduced for the analyses of the coiling process of the hot-rolled strip to consider the temperature effect in simulations. The calculated circumferential strain is compared to experimentally measured data available in the literature [9]. This new approach will be helpful in identifying suitable processing parameters to improve the surface quality under given operation constraints in practice.

2. THEORETICAL MODELING

Similar to the elastic model suggested by Yanagi *et al.* [8], the coil and the new coiling strip were assumed to be thick and thin hollow cylinders, respectively, as shown in Fig. 1(a). In this figure, r_{in} and r_o are the inner and outer radii of the spool, respectively, and r_{max} and w represent the outer radius and half width of the coil, respectively. The coiling tension applied to the thin strip is represented by σ_T. The radial and axial directions are represented by r and z, respectively.

The coiling process was modeled by piling the thick cylinder (the coil) with thin cylinders (the coiling strips) in Fig. 1(a), which were subject to circumferential stress due to the coiling tension. The thick cylinder was then subjected to outer radial pressure, resulting from the circumferential stress in the thin cylinder. During coiling, the incremental stress field within the thick cylinder was determined by using Love's stress function [10]. The stress field within the coil during the coiling process was obtained by applying the principle of superposition of the additional stress field elastically.

In order to consider the axial inhomogeneity of the deformation due to the strip crown, the measured thickness distributions given in Figs. 1(b) and (c), respectively, were utilized in the present analysis. The thickness distribution in the axial direction of the coil in Fig. 1(b) was measured and given by Yanagi *et al.* [9]. The same results were utilized in this study to verify the predicted data by the current theoretical model.

The effects of processing parameters on the formation of flatness defects were investigated using the measured thickness distribution in Fig. 1(c), provided by POSCO, which was fitted as a function of the axial direction z as follows:

$$t(z) = t_0\left[1-\alpha\left(\frac{|z|}{w}\right)^{\eta}\right] \tag{1}$$

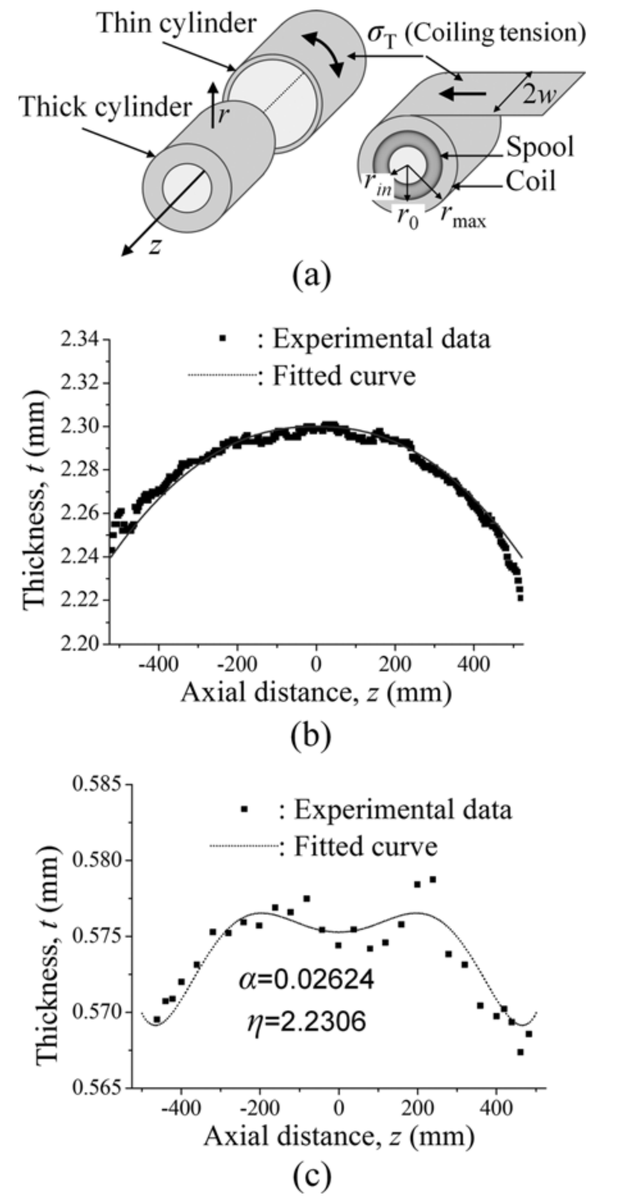

Fig. 1. (a) Schematic diagram of the analytical model for the strip coiling process, (b) measured thickness distribution of the cold-rolled thin-strip [9], and (c) measured thickness distribution of the hot-rolled thin-strip.

where t_0, α, and η are the original thickness, the crown ratio, and the crown index of the strip, respectively.

The outer radius distribution of the coil along the axial direction after winding the new coiling strip on the coil can then be calculated as

$$r_{(n)}(z) = r_{(n-1)}(z) + t(z) + c_{(n)}(z) \tag{2}$$

where n is the number of coiling strips during the coiling process, $r_{(n)}(z)$ is the outer radius of the n-th coiling, and $c_{(n)}(z)$ is the clearance between the coil and the n-th coiling strip.

The circumferential stress distribution in the new coiling strip due to the coiling tension (σ_T) is used to calculate the compressive pressure distribution on the outer lateral surface of the coil. The circumferential stress distribution along the axial direction $\sigma_{\theta 0,(n)}(z)$ can be calculated as follows:

$$\sigma_{\theta 0,(n)}(z) = \frac{E(z)}{1-\nu^2(z)}\ln\left(\frac{2\pi r_{(n)}(z)}{2\pi \bar{r}}\right) \tag{3}$$

where $E(z)$ and $\nu(z)$ are the Young's modulus and Poisson's ratio of the material, respectively. $\bar{r}$ is a representative radius derived from the equilibrium condition of the newly coiled strip, given as

$$\sigma_T \int_{-w}^{w} t(z)dz = \int_{-w}^{w} \sigma_{\theta 0,(n)}(z)t(z)dz \tag{4}$$

As the number of coiling strips increases, the circumferential stress distribution $\sigma_{\theta 0,(n)}(z)$ calculated from Eq. 3 tends to have negative values due to the clearance formed by the strip crown at the edge of the coil. In this case, we change the negative value of $\sigma_{\theta 0,(n)}(z)$ to zero because the value cannot be negative in the strip under coiling tension. The clearance between the coil and the newly coiled strip $c_{(n)}(z)$ can be calculated as follows:

$$c_n(z) = \begin{cases} 0 \ \text{ for } \ \sigma_{\theta 0,(n)}(z) > 0 \\ t(z) - t(z_0) \ \text{ for } \ \sigma_{\theta 0,(n)}(z) = 0 \end{cases} \tag{5}$$

where $r_{(n-1)}(z) + t(z) = \bar{r}$ After determining the circumferential stress distribution $\sigma_{\theta 0,(n)}(z)$ and the representative radius $\bar{r}$, the outer radial pressure applied to the thick cylinder $p_{(n)}(z)$ can be obtained according to the hoop stress equation under the thin-walled approximation introduced to the new coiling strip as

$$P_{(n)}(z) = \sigma_{\theta 0,(n)}(z)\cdot\frac{t(z)}{\bar{r}} \tag{6}$$

The stress components $\sigma_{\theta 0,(n)}(z)$ in the thick cylinder can be calculated using Love's stress function [10] as follows:

$$\nabla^4\Phi = 0, \nabla^2 \equiv \frac{\partial^2}{\partial r^2} + \frac{1}{r}\frac{\partial}{\partial r} + \frac{\partial^2}{\partial z^2}$$

$$\sigma_r = \frac{\partial}{\partial z}\left(\nu\nabla^2\Phi - \frac{\partial^2\Phi}{\partial r^2}\right), \sigma_\theta = \frac{\partial}{\partial z}\left(\nu\nabla^2\Phi - \frac{1}{r}\frac{\partial\Phi}{\partial r}\right)$$

$$\sigma_z = \frac{\partial}{\partial z}\left[(2-\nu)\nabla^2\Phi - \frac{\partial^2\Phi}{\partial z^2}\right], \tau_{rz} = \frac{\partial}{\partial z}\left((1-\nu)\nabla^2\Phi - \frac{\partial^2\Phi}{\partial z^2}\right) \tag{7}$$

In each coiling, boundary conditions for the thick cylinder can be expressed as Eq. 8, neglecting the friction between the new coiling strip and the coil.

$$\sigma_r|_{r=a} = 0, \sigma_r|_{r=b} = -p_{(n)}(z), \sigma_z|_{z=\pm w} = 0, \tau_{rz}|_{r=a} = 0,$$

$$\tau_{rz}|_{r=b} = 0, \tau_{rz}|_{z=\pm w} = 0 \tag{8}$$

where a and b are the inner and outer radii of the thick cylinder, respectively. Yanagi *et al.* [8] introduced the following form of a stress function to calculate the stress distribution within the thick cylinder.

$$\Phi(r,z) = D_0\ln r + F_0\frac{r^2z}{4} + N_0\frac{z^3}{6} + \sum_{n=1}^{\infty}\{A'_n I_0(\beta_n r)$$
$$+ B'_n\beta_n r\cdot I_1(\beta_n r) + A''_n K_0(\beta_n r) + B''_n \beta_n r\cdot(\beta_n r)\}$$
$$\frac{\sin\beta_n z}{\beta_n^3} + \sum_{s=1}^{\infty}\{C_s'\sinh(\gamma_s z) + D_s'\gamma_s z\cosh(\gamma_s z)\}\frac{Z_0(\gamma_s r)}{\gamma_s^3}$$
$$Z_n(\gamma_s r) = Y_1(\gamma_s a)J_a(\gamma_s r) - J_1(\gamma_s a)Y_n(\gamma_s r), Z_1(\gamma_s b) = 0,$$
$$\beta_n = \frac{n\pi}{h} \tag{9}$$

where D_0, F_0, N_0, A'_n, B'_n, A''_n, B''_n, C'_s, D'_s are unknowns of the stress function, J_n and Y_n are Bessel functions, I_n and K_n are modified Bessel functions, and β_n and γ_s are the n-th root of $\sin(\beta_n w) = 0$ and the s-th root of $Z_1(\gamma_s b) = 0$, respectively. To calculate the incremental stress distribution within the thick cylinder $\Delta\sigma_{ij,(n)}(r, z)$, a system of linear equations with the nine unknowns is provided by substituting the stress function $\Phi(r, z)$ of Eq. 9 into each boundary condition in Eq. 8. The stress field within the coil during the coiling process was obtained by Eq. 10 by applying the principle of superposition of the additional stress field.

$$\sigma_{r,(n)}(r,z) = \sigma_{r,(n-1)}(r,z) + \Delta\sigma_{r,(n)}(r,z), \sigma_{r,(n)}(r,z)$$
$$= \sigma_{r,(n-1)}(r,z) + \Delta\sigma_{r,(n)}(r,z)$$
$$\sigma_{\theta,(n)}(r,z) = \sigma_{\theta,(n-1)}(r,z) + \Delta\sigma_{\theta,(n)}(r,z), \tau_{rz,(n)}(r,z)$$
$$= \tau_{rz,(n-1)}(r,z) + \Delta\tau_{rz,(n)}(r,z) \tag{10}$$

First, for verification of the present model, an analysis of the coiling process of the cold-rolled thin-strip was conducted using the same analysis conditions applied by Yanagi *et al.* [9]. The corresponding analysis conditions are given in Table 1 and Fig. 1(b). Second, the effects of processing parameters on the formation of flatness defects of the hot-rolled thin strip during the coiling process were investigated using the analysis conditions, as given in Table 2 and Fig. 1(c). Since the mechanical properties of the hot-rolled strip vary along the axial direction due to the temperature gradient, according to the works by Han *et al.* [11] and Chun *et al.* [12], a temperature-dependent mechanical elastic property is introduced in the present investigation. To consider the influence of the temperature variation along the axial direction on the stress and strain distributions during the coiling process of the hot-rolled strip, the measured temperature provided by POSCO before the coiling is given in Fig. 2(a). In addition, Young's modulus measured by POSCO as a function of the temperature is given

Table 1. Analysis condition of the cold-rolled thin-strip for verification [9]

Inner radius of spool r_{in}	Inner radius of coil r_0	Outer radius of coil r_{max}	Half width of coil w	Thickness of strip t	Coiling tension σ_T	Young's modulus E	Poisson ratio ν
251 mm	255.5 mm	700 mm	500 mm	0.58 mm	20, 40, 80 MPa	200 GPa	0.3

Table 2. Analysis condition of the hot-rolled thin-strip to investigate the effect of processing parameters

Inner radius of spool r_{in}	Inner radius of coil r_0	Outer radius of coil r_{max}	Half width of coil w	Thickness of strip t	Strip crown α	Strip index η	Coiling tension σ_T	Poisson ratio ν
305 mm	375 mm	952 mm	525 mm	2.3 mm	0.026	2.23	25 MPa	0.3

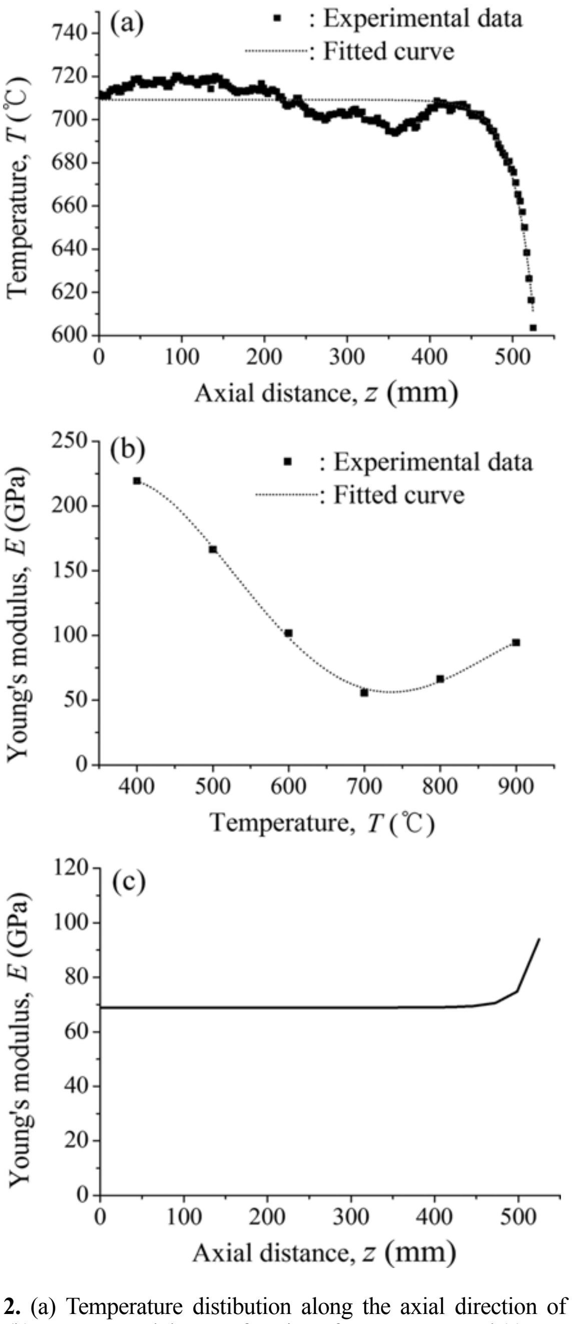

Fig. 2. (a) Temperature distibution along the axial direction of the strip, (b) Young's modulus as a function of temperature, and (c) Young's modulus as a function of axial distance.

in Fig. 2(b). In the same figures, the experimental data were numerically fitted for the present theoretical modeling. Since the coiling time is less than 1 min, it was assumed that the temperature distribution in the coil was not changed during the coiling process. Based on the provided data in Figs. 2(a) and (b), Young's modulus in the axial direction was determined as given in Fig. 2(c). According to this figure, Young's modulus was uniform except for the outer edge of the coil where it was increased because of the temperature drop, as shown in Fig. 2(a).

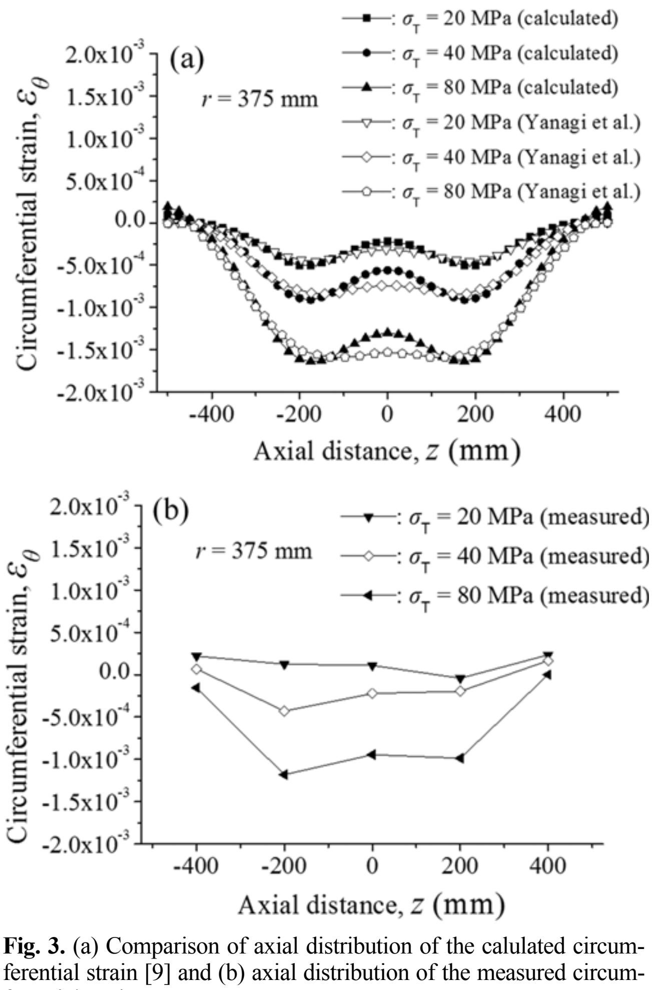

Fig. 3. (a) Comparison of axial distribution of the calulated circumferential strain [9] and (b) axial distribution of the measured circumferential strain.

3. RESULTS AND DISCUSSION

For verification of the present theoretical modeling, the experimental data provided by Yanagi *et al.* [9] were calculated using the same processing conditions as given in their study. In Fig. 3, the calculated circumferential strain distribution along the axial direction is compared with the measured and predicted distributions in Yanagi *et al*. [9]. There is a slight difference between Yanagi *et al.*'s prediction and the present data, as shown in Fig. 3(a). Since the measured thickness distribution given in Fig. 1(b) was used in the analysis, the double peak pattern of circumferential strain distribution was also captured in the measured distribution in Fig. 3(b). The compressive circumferential strain increased as the coiling tension increased in the central region of the axial direction while the strain level was almost unchanged at the edge part. From this comparison, it can be construed that the currently developed numerical model can predict the deformation mechanics of the thin-strip coiling process with reasonable accuracy.

In order to better understand the formation of flatness defects, the theoretical model was applied to determine the effect of processing parameters involved in the strip coiling process. In Fig. 4, radial and circumferential stress distributions are compared along the radial and axial directions. Figure 4(a) shows that tensile and compressive stresses occurred at the outer and inner strips, respectively. This figure indicates that compressive stress accumulates as the coiling process proceeds due to the coiling tension. In Fig. 4(b), the stress distribution along the axial direction is shown. This figure is helpful in understanding the underlying mechanism of flatness defects in the strip. At the outermost strip ($r = 952$ mm), only the central region of the axial direction is subject to tensile circumferential stress. The stress concentration is attributed to the strip crown, which might cause concentrated contact between the coiling layers of the strip. Such inhomogeneity of the circumferential stress distribution along the axial direction could result in a center buckle in the outer strip ($r > 450$ mm). At the innermost strip ($r = 375$ mm), however, most regions except for the edge is subject to compressive circumferential stress. Although the strip is subject to tensile stress at the initial stage of the coiling process, compressive stress accumulates within the strip as the coiling process proceeds due to the pressure resulting from the coiling tension appiled to the

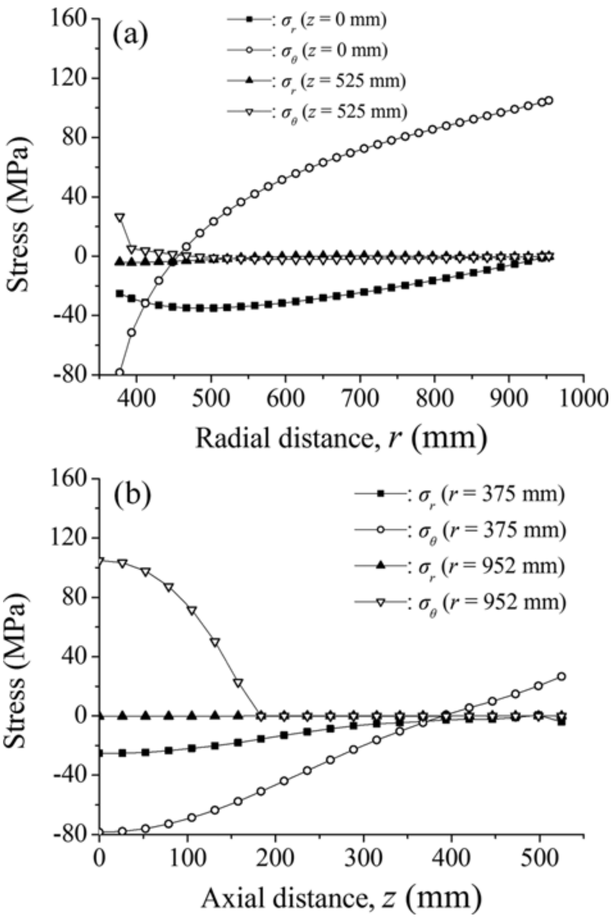

Fig. 4. Radial and circumferential stress distributions along (a) the radial and (b) the axial direction.

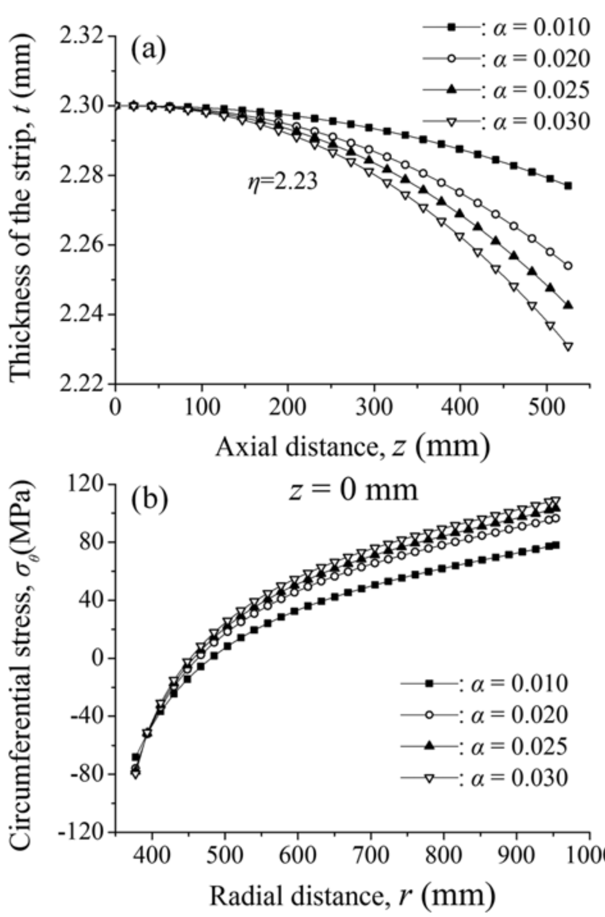

Fig. 5. (a) Thickness distribution of the strip and (b) circumferential stress distribution depending on the crown ratio α.

outermost strip. In particular, accumulation of the compressive stress is concentrated at the middle of the axial direction owing to the strip crown. Such inhomogeneity of the circumferential stress distribution along the axial direction could result in an edge wave at the inner strip ($r < 450$ mm).

In Fig. 5, variation of the thickness distribution of the strip and the corresponding circumferential stress distribution are shown depending on the crown ratio α only since the effect of the crown index η is negligible. As the crown ratio α decreases, the magnitude of the circumferential stress within the overall region of the coil decreases as well, resulting in a less inhomogeneous stress distribution. This means that it is necessary to reduce the strip crown as much as possible to prevent the formation of flatness defects. However, the formation of the strip crown in the hot rolling step prior to the coiling process is inevitable. Therefore, it is necessary to find a way to reduce the flatness defects through investigation of the effects of the controllable processing parameters associated with the coiling process.

The effect of the coiling tension on the stress distribution is illustrated in Fig. 6. As the coiling tension decreases, the magnitude of the circumferential stress in the overall region of the coil decreases as well, resulting in a less inhomogeneous stress distribution. In particular, with around a 30% reduction in the coiling tension, the magnitude of the circumferential stress is decreased by about 30% in the inner strip, where the edge wave is readily formed. Thus, lowering the coiling tension might be an effective means of preventing the formation of flatness defects. However, there is a limit to how much the coiling tension can be lowered, because a certain minimum level of coiling tension is required to make the process feasible in practice.

Additional analyses were conducted to calculate the stress distribution under varying coiling tensions. In order to reduce the level of the compressive circumferential stress in the inner strip, coiling tension with a transient increase at the beginning stage of the coiling process is introduced in the present study. This strategy was conceived based on the hypothesis that the increased tensile stress due to the transient increase of the coiling tension at the initial stage only would counterbalance the accumulated compressive stress.

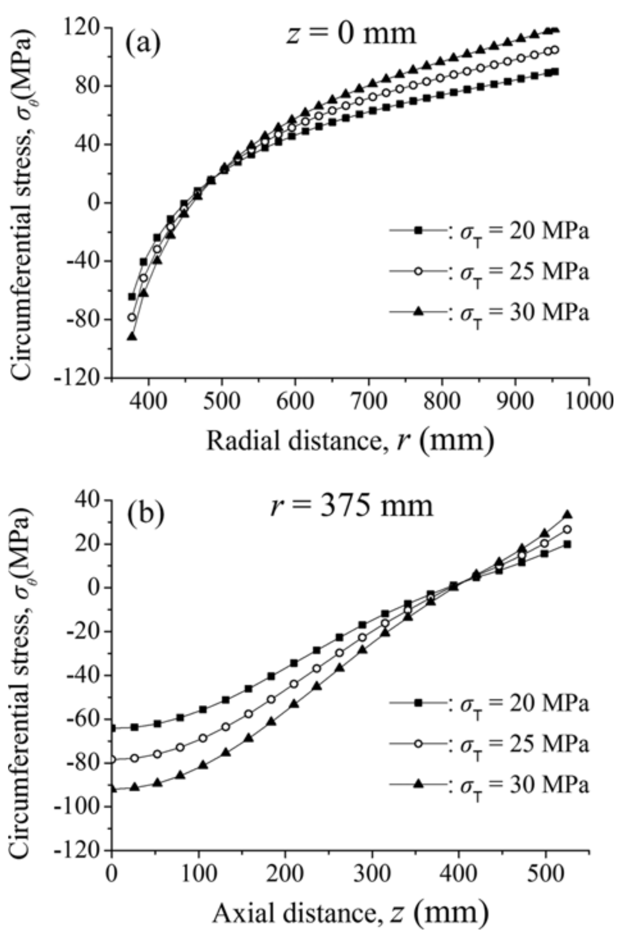

Fig. 6. Circumferential stress distributions along (a) the radial and (b) the axial directions depending on the coiling tension, respectively.

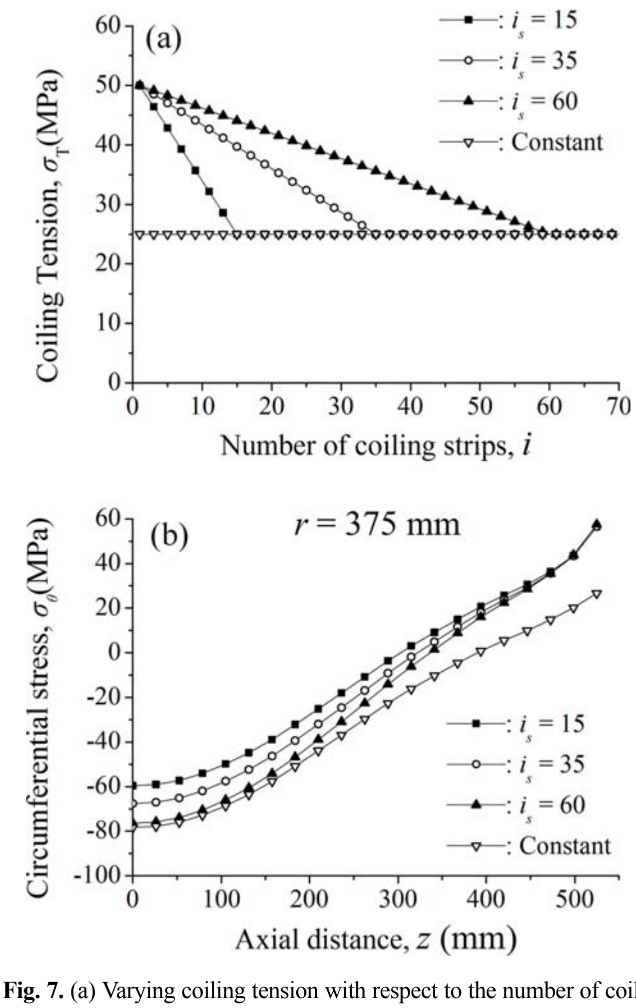

Fig. 7. (a) Varying coiling tension with respect to the number of coiling strips and (b) circumferential stress distribution depending on the pattern of the coiling tension.

In Fig. 7(a), the pattern of the varying coiling tension is shown. The varying coiling tension starting with an initial value of 50 MPa was set to decrease linearly with respect to the number of coiling strips until the i_s-th coiling and then remained constant. The results in Fig. 7(b) confirm the hypothesis. In particular, it is noticeable in this figure that the duration of the transient increase of the coiling tension should be as short as possible.

The effect of the spool thickness on the stress distribution is illustrated in Fig. 8. As the spool thickness increases (or r_{in} decreases), the magnitude of the circumferential stress in the inner strip decreases significantly, resulting in a less inhomogeneous stress distribution. In particular, the magnitude of the circumferential stress in the inner strip decreased by around 50% while it was not significantly affected in the outer strip. Thus, increasing the spool thickness may be a good strategy for prohibiting the formation of the edge wave in the inner strip.

Similar to the strip crown described in Eq. 1, the spool crown is introduced in this study by assuming the spool crown height α_b and index η_b due to thermal expansion, wear, and elastic deformation. In this regard, it is worth investigating the effect of the spool crown on the stress distribution. The thickness distribution of the spool depending on the spool crown height α_b is depicted in Fig. 9(a) and the corresponding circumferential stress distribution is given in Fig. 9(b). With the increase in the spool crown height α_b, the level of the compressive circumferential stress in the inner strip was greatly reduced, resulting in a less inhomogeneous stress distribution. Specifically, the compressive circumferential stress decreased by around 50% at the middle of the axial direction when the spool crown height α_b increased up to 1.3 mm. For further increase of the spool crown height ($\alpha_b = 2.0$ mm), the compressive circumferential stress rather increased in the central region of the axial direction ($z < 250$ mm). This result indicates that imposing an artificial spool crown might be a good strategy for reducing the flatness defects.

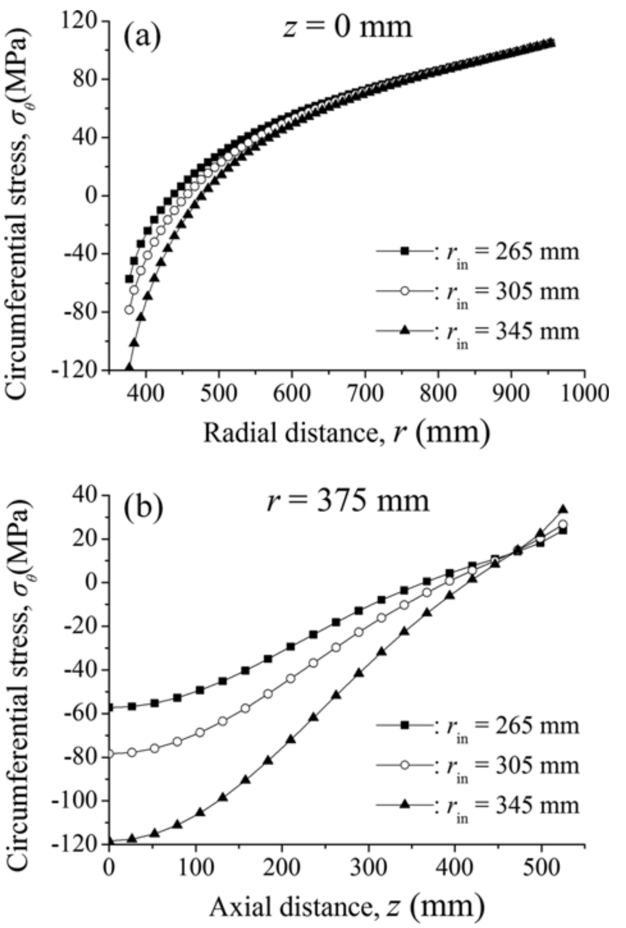

Fig. 8. Circumferential stress distributions along (a) the radial and (b) the axial directions depending on the thickness of the spool.

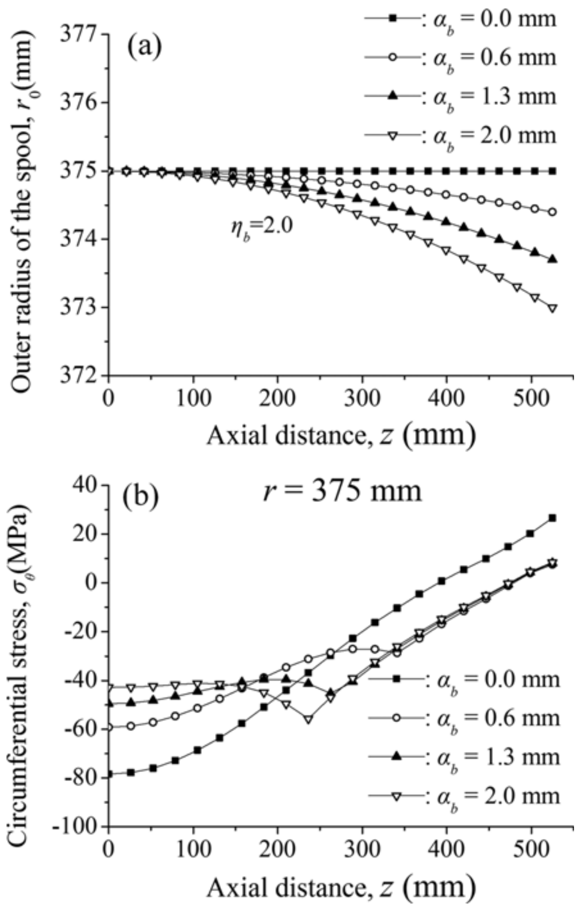

Fig. 9. (a) Thickness distribution of the spool and (b) circumferential stress distribution depending on the spool crown height α_b.

4. CONCLUSIONS

In the present study, the influences of processing parameters such as strip crown, spool geometry, and coiling tension on the stress distribution in the strip during the coiling process were investigated by using an analytical model to determine the elastic stress distribution and deformation. According to the present analysis, it was found that the strip flatness can be improved by suppressing the strip crown, increasing the thickness of the spool with the shape of a swollen hollow cylinder, and lowering the coiling tension with a transient increase at the beginning stage of the coiling process only. In particular, the compressive circumferential stress was decreased by around 50% when either the spool thickness was increased by around 3.5 times or the spool crown height α_b was increased up to 1.3 mm in the inner strip, resulting in a less inhomogeneous stress distribution. The finding of this study might be informative in reducing the formation of the edge wave in the inner strip during the coiling process.

ACKNOWLEDGMENT

This work was made possible through support by POSCO.

REFERENCES

1. J. Y. Jung and Y. T. Im, *J. Mater. Proc. Technol.* **63**, 248 (1997).
2. J. Y. Jung and Y. T. Im, *J. Mater. Proc. Technol*. **96**, 163 (1999).
3. T. Kawanami, T. Asamura, and H. Matsumoto, *J. Mater. Proc. Technol.* **22**, 257 (1990).
4. H. C. Kwon, I. S. Han, and M. S. Chun, *Proc. 10th Int. Conf. Techn. Plast.* (eds. G. Hirt and A. E. Tekkaya), p.37, WTH Aachen University, Aachen, Germany (2011).
5. R. B. Sims and J. A. Place, *Br. J. Appl. Phys.* **4**, 213 (1953).
6. D. B. Miller and M. Thornton, *Proc. 5th Int. Rolling Conf.* (ed. M. C. Gleave), p.73, Institute of Metals, London, United Kingdom (1990).
7. A. A. Sarban, *Proc. 2nd Int. Conf. on Modelling of Metal Rolling Proc.* (eds. Beynon JH, Ingham P, Teichert H, and Waterson K), p.92, Institute of Materials, London, United Kingdom (1996).
8. S. Yanagi, S. Hattori, and Y. Maeda, *J. JSTP* **39**, 51 (1998).
9. S. Yanagi, S. Hattori, Y. Maeda, H. Ibata, Y. Sugimoto, and M. Sawada, *Proc. 7th Int. Conf. on Steel Rolling*, p.150, Iron and Steel Institute of Japan, Chiba, Japan (1998).
10. A. E. H. Love, *A Treatise on the Mathematical Theory of Elasticity*, *4th. ed.*, pp.274-276 , Dover Publications, New York (1944).
11. S. Han, H. Seong, Y. Ahn, C. I. Garcia, A. J. DeArdo, and I. Kim, *Met. Mater. Int.* **15**, 521 (2009).
12. E. J. Chun, J. S. Lee, H. H. Do, S. J. Kim, Y. S. Choi, Y. H. Park, and N. H. Kang, *Korean J. Met. Mater.* **50**, 487 (2012).